





Fault Diagnosis of Voltage Source Inverter using Quadrant Transformation and Pattern Recognition

^{1st}R. B. Dhumale ^{1*}, ^{2nd}Ajay K. Dass , ^{3rd}Anshika Singh , ^{4th}Gaurav Raskar 

¹ AISSMS Institute of Information Technology, Pune, India.

² Sinhgad College of Engineering, Pune, India.

³ AISSMS Institute of Information Technology, Pune, India.

⁴ AISSMS Institute of Information Technology, Pune, India.

*Corresponding Author: rbd.scoe@gmail.com

ARTICLE INFO

Received: 28 Dec 2024

Revised: 14 Feb 2025

Accepted: 26 Feb 2025

ABSTRACT

This work purposes to address the need for open switch fault diagnosis in 3-phase voltage source inverters used in industry, with the goal of enhancing consistency, minimizing downtime, reducing maintenance costs, and ensuring optimal performance. Open switch faults in switching devices can considerably reduce the efficacy as well as consistency of a voltage source inverter. This leads to costly downtimes and increases security risks. This paper proposes a novel technique for open switch fault diagnosis that consists of feature extraction, rule-based modeling, as well as machine learning and pattern recognition in fault diagnosis with the combination of direct-quadrant transformation and convolutional neural networks. This technique successfully detects faulty switches by integrating direct-quadrant transformation, feature selection, as well as fault classification. The direct-quadrant transformation aids in distinguishing between healthy as well as defective states by mapping signals into different patterns. These patterns are then improved after feature selection, increased diagnostic accuracy, and machine learning-based fault identification, resulting in reliable and efficient diagnoses. Two methods for open switch fault diagnosis utilized in the paper are pattern recognition and fault diagnosis using a feature-based fault diagnosis system. A feature-based fault diagnosis system uses rule-based as well as machine learning models for fault classification, subsequently extracting features from direct-quadrant transformed data as well as selecting appropriate features. Convolutional neural networks with pattern recognition methods are applied in fault diagnosis to transform direct-quadrant transformed input images. These methods were compared on the basis of robustness, computational efficiency, as well as diagnostic accuracy in many operating conditions.

Keywords: Three-Phase Voltage Source Inverters, Open Switch Faults, Direct Quadrant Transformation, Pattern Recognition

INTRODUCTION

The systems like Electric grids, industrial machinery and renewable energy depend on inverters to convert direct current (DC) into alternating current (AC) (Amol Rathod *et al.*, 2022). AC is preferred over DC for long-distance transmission because it is easier to step up or step down the voltage using a transformer, which reduces energy loss over long distances. A 3 phase voltage source inverter (3 Φ -VSI) produces a three-phase, adjustable sinusoidal waveform. Controllable sinusoidal waveforms are required for power quality control and load balancing in grid and industrial applications. Waveform controllability enables precise voltage and frequency changes, which are essential for smooth power transfer, effective motor performance and reduced harmonic distortion. The output waveform of an inverter can be distorted by electrical noise, which is introduced by frequent switching transients, power supply variations, or external electromagnetic interference. This results in harmonic distortion, which affects system performance by increasing heat in components, causing vibrations in motors and reducing the overall efficiency and lifespan of connected equipment (Dhumale *et al.*, 2024). However, 3 Φ -VSI switching devices, such as metal oxide field effect transistors (MOSFETs) and insulated gate bipolar transistors (IGBTs), are prone to errors such as open switch errors (OSFs) and short circuit faults (SCFs) (Sonawane, 2022). IGBTs are designed to withstand SCFs for a certain period of time to protect the device from SCFs. An IGBT can usually withstand SCF for 5-10 μ s (Basler *et al.*, 2013).

This period is critical because it allows the protective circuitry to detect the problem and begin the process of shutting down the IGBT and preventing it from failing. The thermal and electrical limitations of IGBTs are the reason for this small tolerance window; If the SCF continues beyond this point, excessive current can inevitably damage the device. Because the fault must be identified and resolved in order to activate protective mechanisms such as circuit breakers or shutdown protocols to stop damage and guarantee continuous safe operation of the inverter, this tolerance period is essential for fault detection and protection circuit design. Several strategies are used to protect against SCF and to guarantee that the switching devices do not experience any short circuits. Fast-acting fuses cut off large fault currents before they can damage the device, while desaturation detection circuits track the collector-emitter voltage of IGBTs to quickly identify overcurrent conditions. Furthermore, gate drivers with integrated protection features have the ability to immediately stop the IGBT when a fault is detected, thereby increasing device life and preventing ongoing problems. Comparison of the current signal to a predetermined threshold can be used to identify SCFs, but more efficient methods are needed to diagnose OSF (Wu and Zhao, 2016). Monitoring OSFs is critical for ensuring system reliability and safety. The output voltage and current can become uneven because of these faults, which can also lower efficiency and do a lot of damage to the load connected to the VSI (Farooqi et al., 2022). Timely diagnosis of OSF is serious to protect operational instability, save downtime, and defend equipment.

For VSI, various **Fault Diagnosis Methods (FDMs)** have been suggested; all FDMs propose distinctive methods to isolate OSF. Diagnosing various OSFs in a PMSM method is significant to reduce torque imbalance, efficiency loss, as well as overheating, and to assure accurate, dependable performance in needed applications. The technique (Chen et al., 2019) concentrates on diagnosing multiple OSFs in a **Permanent Magnet Synchronous Motor (PMSM)** drive system by way of an average **Fault Isolation Time (FIT)** of 1.7 ms. Threshold free single OSF diagnosis in a multilevel inverter is the concentrate of the technique using **Discrete Wavelet Transform (DWT)** as well as **Machine Learning (ML)** algorithms with FIT ranging from 0.433 seconds to 0.502 seconds (Achintya and Kumar Sahu, 2020). The technique (Gong et al., 2020) practices **Convolutional Neural Networks (CNNs)** to accurately diagnose IGBTs in DC-DC converters with fast training as well as testing times. One-third of the cycle time is the time needed for diagnosis by the technique (Chen et al., 2021), which applies an **Extended State Observer (ESO)** to diagnose OSF in stages. For example, if the AC signal cycle is 20 milliseconds, the ESO will take about 6-7 milliseconds to diagnose. Diagnostics must be finished inside fractions of cycle time to guarantee a steady and unremitting process of the system, reduce downtime, and remove faults quickly.

The **Total Harmonic Distortion (THD)** characteristics are utilized to design a **Fuzzy Logic (FL)** system for OSF diagnosis with a diagnosis time as short as 32 ms (Chen et al., 2021). The FL technique is essential to achieve the uncertainty as well as ambiguity in THD data. FL system-based FDMs provide quick and correct diagnosis needed to keep inverter stability with less downtime. The OSF diagnosis technique for six-phase AC-DC wind turbines with a diagnosis time of 0.14 seconds is proposed in (Mehta, Sahoo and Dhiman, 2022). The method suggested in (Bengharbi et al., 2023) used for single as well as multiple OSF diagnosis of photovoltaic solar pumping systems, gives **Artificial Neural Network (ANN)** as well as **Adaptive Neuro Fuzzy Interface System (ANFIS)** with high accuracy and a response time of less than 0.1 seconds. ANN-based OSF diagnosis in a HANPC inverter has been proposed to attain a diagnosis time of 0.11 seconds with a low minimum dependency on the threshold value (Abid et al., 2022). A real-time bagged tree, which is fast, easy to understand, and reliable, was proposed for OSF diagnosis in 3 Φ -VSI by Jian-Jian and Zhang (Wu and Zhao, 2016) with an isolation time of approximately 4 ms.

The few methods implemented for OSF diagnosis are inadequate and show variations in terms of installation difficulty, diagnosis time, and accuracy, while other methods diagnose faults with better accuracy, which is significant to minimize false positives and negatives. Furthermore, diagnosis times are not the same, with certain techniques showing high latency while others techniques provide real-time fault diagnosis. Additionally, the effort required for implementation differs extensively; complex systems need considerable computing resources with fine-tuning for maximum performance. However, simple systems require less processing and tuning. **Artificial intelligence (AI)**-based methods have accuracy as well as effectiveness; however, because of their complexity, they can compromise implementation effort plus diagnosis time. Traditional methods with threshold reliance, in comparison, may be to a smaller degree flexible, not so much resistant to load variations, and rarely able to diagnose many OSFs, as found in the literature.

This paper suggests a new method to address this inconsistency by combining the best qualities of threshold dependent and AI-based systems to minimize threshold dependency, high implementation effort, and heterogeneous diagnosis times. It tries to attempt an additional practical and effective method to diagnose OSF. Within the framework of the condition-based maintenance (CBM) paradigm of Industry 5.0, this work efforts on diagnosing OSF. The proposed

approach compares **Pattern Recognition (PR)** approaches with statistical feature-based techniques plus image recognition methods to confirm reliable OSF diagnosis in 3 Φ -VSI systems.

This includes feature extraction using Direct Quadrant (DQ) transformation and feature selection to detect various fault states with healthy operation. The technique improves power electronic converter dependability by lowering threshold dependence, diagnosis time, and implementation effort while also increasing robustness. AI and PR techniques guarantee reliable, low-maintenance performance in power-dependent regions by enabling precise problem diagnosis in a variety of scenarios.

MATERIALS AND METHODS

A 3 Φ -VSI has six switches, S1, S2, S3, S4, S5 and S6, as shown in Fig. 1, these switches are turned on and off in such a way that the output of the 3 Φ -VSI is in the form of a sine wave as shown in Fig. 2. When the switches are turned on, currents I_a , I_b and I_c flow continuously, indicating a healthy condition. In OSF fault condition output current I_a , I_b and I_c flow is disturbed as shown in Fig. 3. An OSF occurs when one or more switches malfunction, interrupting the current flow of the affected phase. As a result, there is an imbalance, the current in the problematic phase drops to zero while the other phases either remain the same or fluctuate in strength. As the inverter tries to compensate, the current waveforms distort, exhibiting spikes and abnormalities. The control system reacts without fully compensating for the loss, increasing the voltage on the remaining phases. The reliability of power electronic converters and associated loads is ultimately compromised by this imbalance, which also reduces operational efficiency and increases the likelihood of overheating or failure of the remaining components. The proposed methodology for OSF diagnosis in a 3 Φ -VSI has been divided into three major parts, as shown in Fig. 4.

- A. Pattern Generation for healthy and faulty condition
- B. Fault Diagnosis using Statistical Features (FDSF)
- C. Fault Diagnosis using Pattern Recognition (FDPR)

In this system, the process started by creating samples representing healthy and faulty conditions of the system. Data was collected from the system during both normal and malfunction operations, using techniques including sensor measurements, data gathering equipment and logging software. These data were then transformed using the DQ transformation, a mathematical technique that helps to clearly distinguish between different faulty conditions. As a result, distinct patterns representing the behavior of the system at each condition were formed. These generated patterns were then used in two different fault diagnosis methods. Each method uses samples to analyze and identify whether the system is operating under healthy condition or has a fault. By comparing the current state of the system with the generated patterns, the methods can accurately diagnose the state of the system and detect any faults that may have occurred.

The first method which is FDFS, extracts features from the generated patterns. The mean of these features was calculated, then the features were selected and the selected features were used to develop a model using If-Then Rules and ML to diagnose defects. Another method is FDPR. This method requires further processing of the generated samples for fault diagnosis. The generated patterns using DQ transform were converted into images and analyzed using pattern recognition techniques. Different ML based algorithms are implemented and evaluated using extracted features. Several machine learning techniques, including as SVM, decision trees, random forests, KNN, neural networks and gradient boosting, are employed to leverage the collected features for improved fault diagnosis.

Also the images are used to develop **Convolutional Neural Networks (CNNs)** to classify healthy and faulty switches.

A. Pattern Generation for healthy and faulty condition:

During the data acquisition phase, current samples were carefully collected to capture the behavior of the system under various faulty conditions, with special emphasis on single OSFs and multiple OSFs scenarios. For this purpose, a comprehensive dataset was created that included 11 different combinations of fault conditions. This

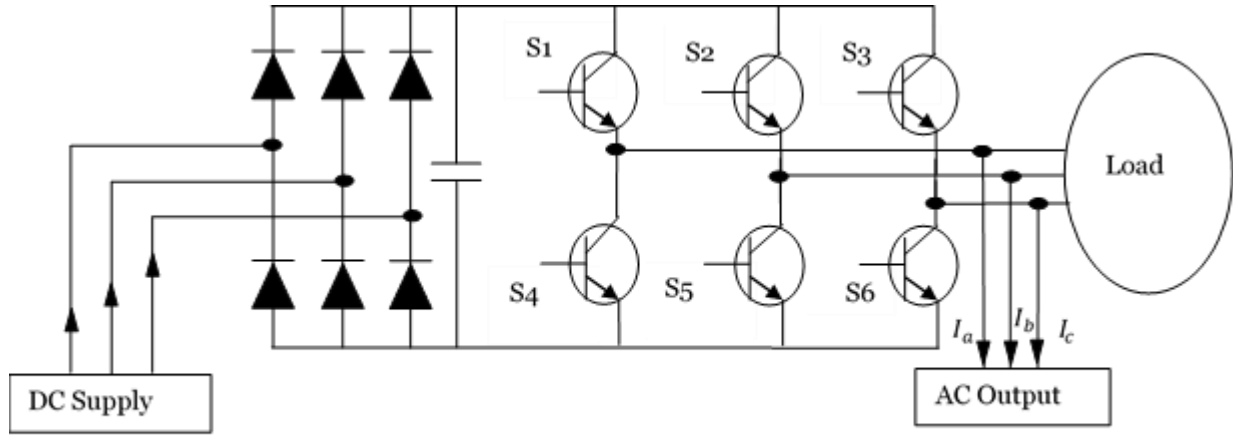


Fig. 1. 3Φ-VSI model

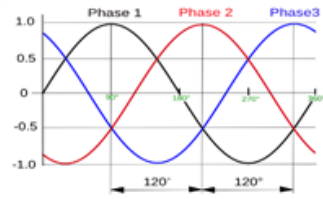


Fig. 2. Healthy Current Output

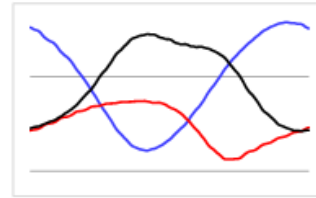


Fig. 3. Distorted Current Output of OSF

combination was created by sequentially opening each switch to simulate a single OSF and then opening pairs of switches to represent multiple OSFs. A large dataset of 8000 samples was generated for each fault condition, ensuring robust and representative data for further analysis. Data transformation was the next step in the pattern generation pipeline. The collected 3Φ current inputs were transformed into 2 attributes using the DQ transformation. The DQ transformation reduces the dimensionality of the data from three to two elements, which makes data processing easier, improves signal clarity and makes fault detection algorithms easier to use for efficient monitoring.

The currents I_a , I_b and I_c in the AC output shown in Fig 2 and Fig 3 are converted into I_d and I_q . The characteristics I_d and I_q were obtained using the mathematical formulas given in Eq 1 and Eq 2. Samples for each switch position were generated by plotting on the I_d -axis and I_q -axis, respectively.

$$I_d = \sqrt{\frac{2}{3}} I_a - \frac{1}{\sqrt{6}} I_b - \frac{1}{\sqrt{6}} I_c \quad (1)$$

$$I_q = \frac{1}{\sqrt{2}} I_b - \frac{1}{\sqrt{2}} I_c \quad (2)$$

The comprehensive data includes one sample representing the healthy condition and 10 samples corresponding to the faulty conditions. Upon closer inspection, distinct differences between these patterns became apparent. The ultimate goal of the model was to determine whether these terms could be used directly for further analysis, or if alternative feature selection procedures were needed to enhance the performance of the model.

B. Fault Diagnosis using Statistical Features:

The initial condition of the switches was set to 'healthy,' where all switches operate under healthy conditions, yielding a pure 3Φ current output. The feature selection process involves the computation of 5 data samples from each generated pattern after DQ transformation, as shown in Fig 5.

First, the co-ordinates of the Centroid (G) of pattern were calculated using median formulas. Then, the co-ordinate axes were shifted to the centroid and the intersection of co-ordinate axes to the locus of the generated pattern was calculated with points as shown in Fig. 6 and Fig. 7. The process of random sampling for OSF and selection of further features, which are required for efficient fault detection, are shown in Figures 6 and 7. This technology improves the accuracy of machine learning models for identifying problems with power electronic systems. The Centroid G , given by

Eq. 3. It acts as the center of attention for the data, emphasizing variations and simplifying analysis to find patterns and faultss.

$$Centroid(G) \equiv (x_m, y_m) \quad (3)$$

The origin was shifted to the centroid G to obtain the points of intersection between the locus of the generated pattern and the translated axes, namely $P_{(1)}$, $P_{(2)}$, $P_{(3)}$, and $P_{(4)}$ calculated using **Eq. 4**, **Eq. 5**, **Eq. 6** and **Eq. 7** respectively. Determining the centroid and intersection points provides important insight into the operational state of the system.

$$P_{(1)} \equiv (x_m, y_2) \quad (4)$$

$$P_{(2)} \equiv (x_m, y_1) \quad (5)$$

$$P_{(3)} \equiv (x_1, y_m) \quad (6)$$

$$P_{(4)} \equiv (x_2, y_m) \quad (7)$$

The median (x_m), given by **Eq. 8**.

$$x_m = Med(X) = \begin{cases} X \left[\frac{n+1}{2} \right] & \text{if } n \text{ is odd} \\ \frac{X \left[\frac{n}{2} \right] + X \left[\frac{n}{2} + 1 \right]}{2} & \text{if } n \text{ is even} \end{cases} \quad (8)$$

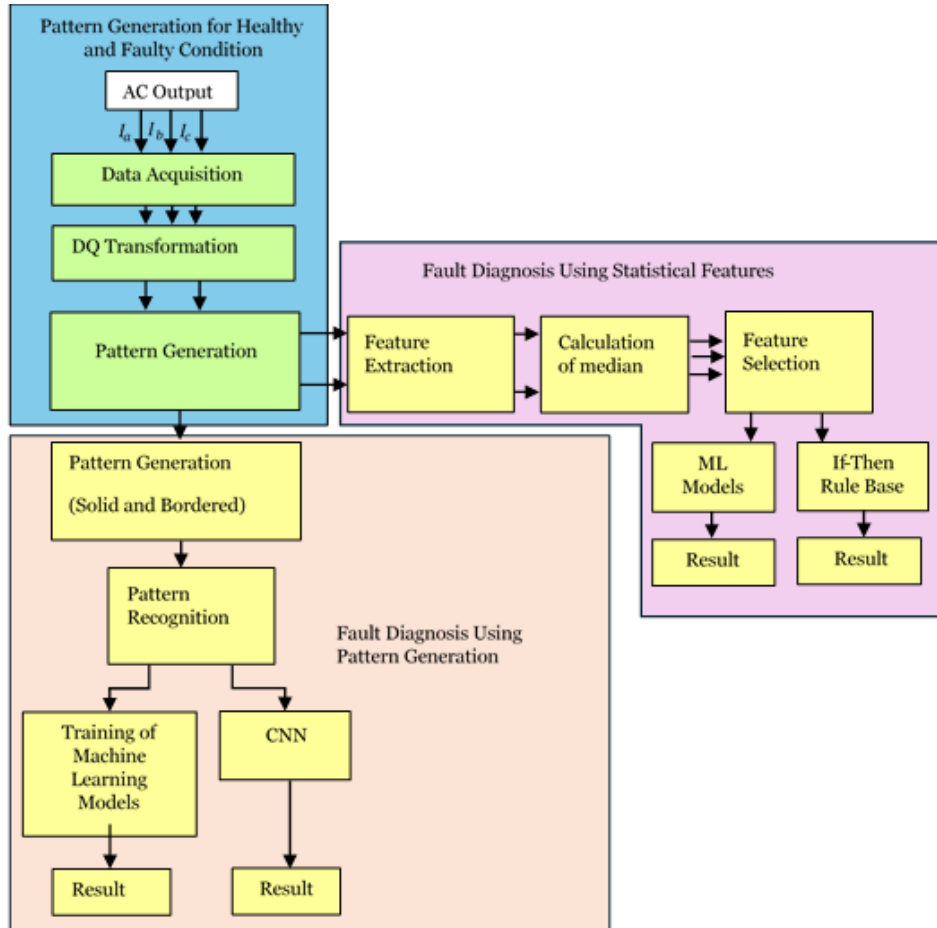


Fig. 4. Proposed Methodology for Diagnosis of Open Switch Faults in Power Converter Converters

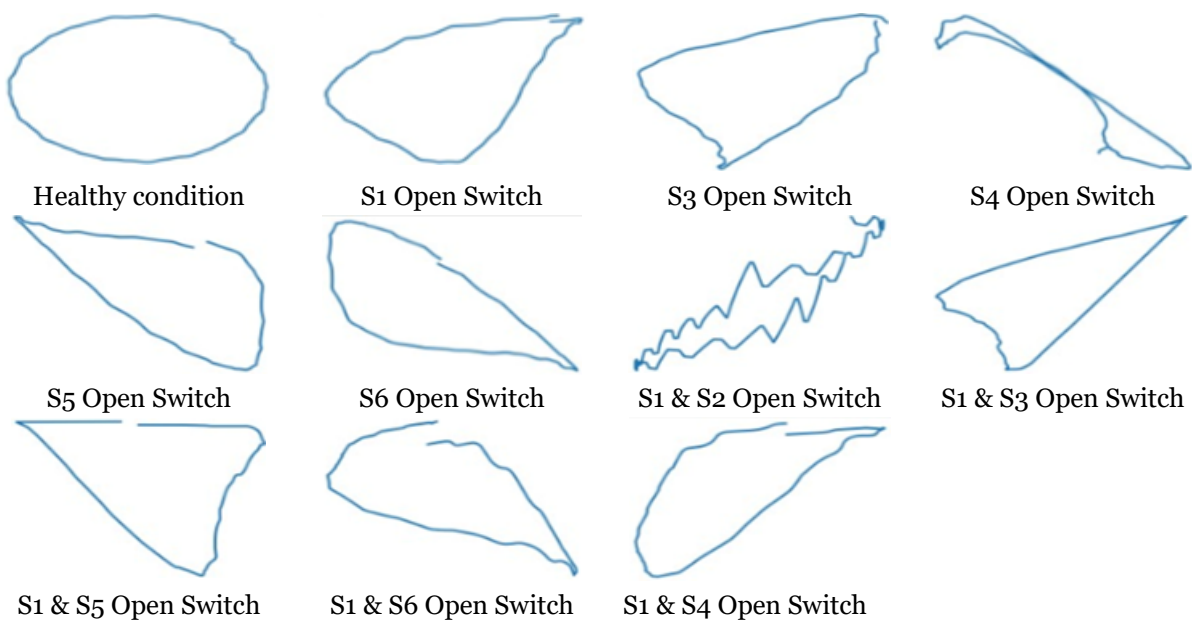


Fig. 5. DQ transformation Generated Patterns

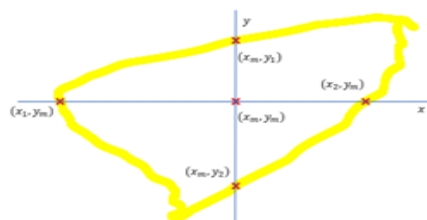


Fig. 6: Random generated Pattern for OSF

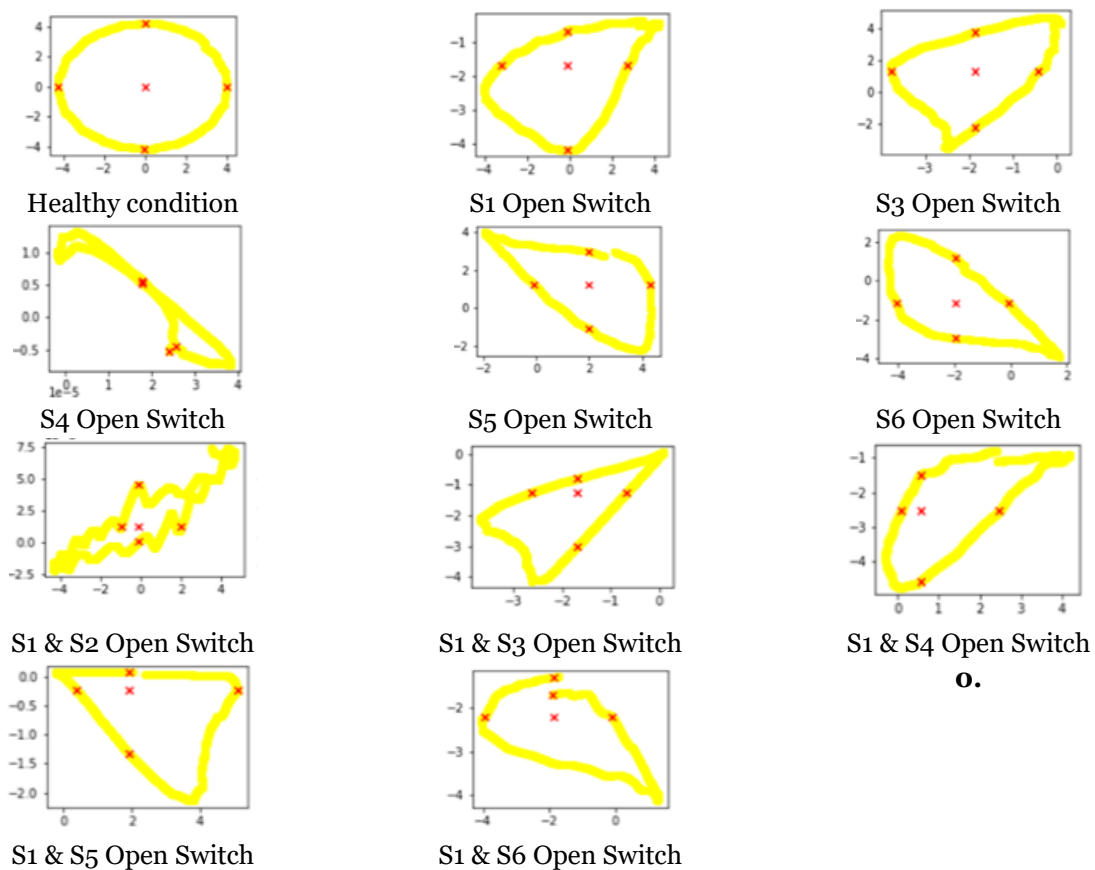


Fig 7: Feature Selection from Generated Patterns

Where X is the ordered list of values in the dataset I_q and n is the number of values in the dataset I_q . Where Y is the

ordered list of values in the dataset I_d and n is the number of values in the dataset I_d . The value x_m in Eq. 4 represents the value of I_d which helps to determine the abscissas of the centroid and the points of intersection between the locus of the generated pattern and the translation axes. If the locus of the given plot curve follows, $y = f(x)$ Then, y_1 & $y_2 = f(x_m)$ and x_1 & $x_2 = f(y_m)$. The features were selected for pattern recognition and stored as a Feature Vector Table as shown in Table 1.

After the feature selection process, the ML models were trained using the feature vectors listed in Table 1. Features were simplified into datasets with 'x' and 'y' coordinates along with their corresponding class labels to facilitate easy classification. A variety of ML algorithms were selected, including **Support Vector Classifier (SVC)**, linear and non-linear polynomial (degree 3) kernels, Naïve Bayes with Gaussian function and Random Forest classifier. These methods equipped distinctive benefits that improved the overall efficiency of FDM. Primary fault classification tasks significantly benefit from the computational efficiency as well as effectiveness of linear SVCs in high-dimensional domains. Model fit and fault diagnosis accuracy were improved using complex relationships in the data, which were detected by non-linear SVC with polynomial kernels. As a result of its strong probabilistic foundation plus user-friendliness, the Naïve Bayes algorithm with Gaussian function was selected. It offers fast and effective fault diagnosis in real time and works best with widely dispersed features. The random forest classifier controlled complex feature interactions with flexibility and reliably implemented well with immaterial or noisy features by merging numerous decision trees to avoid over-fitting and boost classification accuracy.

Using the benefit of each model for robust as well as reliable fault diagnosis, this method combines multiple models to generate a comprehensive and effective FDM. To diagnose OSF in 3Φ-VSI, the data were classified into different fault states using the "If-Then Rule Base" technique. Data with features like median_x, median_y, points_x1, points_y1, points_x2, points_y2, points_x3, points_y3, points_x4 and points_y4 were used in this method from Table 1. Table 1 details the 3Φ-VSI system, which is an important resource for understanding feature vectors used in OSF diagnostics. They benefit in pattern recognition, increase detection sensitivity, and give a detailed representation of working situations. These points were adopted for their empirical significance, potential to do better diagnostic accuracy, and data-driven study to guarantee that the model successfully differentiates among healthy and defective states. This careful feature selection contributes to the ultimate goal of accurate fault diagnosis.

The "if-then rule basis" method make simple the method of fault diagnosis because the selected features offer significant information about the system's implementation. By strengthening the overall diagnostic capability, this structured representation improves system reliability and fault management.

Table 2 signifies a healthy and different faulty conditions that was assigned a class label. This consist of the 'healthy_data' state as well as other OSF states designated 'open1' to 'open16'. A series of conditional statements that evaluated these attributes then identified the output class that formed the rule base. By using different feature values, the scenario helped in the classification of different defect categories. Table 2 shows the rule base.

For clarity, the mathematical notation is displayed in tabular form. An "if-then rule base" is used to diagnose OSF in 3Φ-VSI systems, highlighting the importance of thresholds for distinguishing operational modes. These thresholds, which are determined through statistical analysis, experimental calibration and machine learning techniques, ensure the accuracy and reliability of the rules. Fault diagnosis are intended to increase system performance and reliability by improving diagnostic performance, optimizing decision-making, and adapting to changing operational conditions. As shown in Figure 8, FDPR is implemented using a convolution neural network (CNN) model that begins with data augmentation of various OSF patterns in order to generate images for each class. A strategic method to improve fault diagnosis capability is the use of FDPR with a CNN model initialized with data augmentation. In addition to improving model generalization, reducing overfitting, and simulating real-world variability, data augmentation solves problems associated with limited data availability. As a result, 3Φ-VSI operate reliably due to a more robust and efficient problem diagnosis mechanism. As shown in Fig. 8, the images generated for each OSF class play an important role in the training process, allowing the CNN to accurately identify and classify a range of fault events. This phase improved the dataset and allowed the model to generalize to fault scenarios that had not been encountered before by producing many permutations of the original data. Then, in order to build the model, complimentary data pre-processing was done, which included normalization and conversion to scaled array format. This preprocessing phase ensured that the data was in the right format and scale, which was essential for neural network training to be successful. 50 neural network layers ResNet-50 was a distinct pretrained model whose capability was superior by transfer learning. ResNet-50 was selected because of its potent feature extraction capabilities, which significantly improve the features utilized in the model development stage. ResNet-50 was precisely selected because of its deep learning abilities, innovative residual

learning architecture, recognized performance in image classification tasks, and best suitability for transfer learning. Fault diagnosis with pattern recognition leverages ResNet-50's ability to learn complex 3Φ -VSI characteristics, adapt to specific diagnostic tasks, and locate open switch faults (OSFs) with high accuracy. This choice increases the overall effectiveness and reliability of the fault diagnosis process.

After preprocessing and augmentation, the processed data was scrutinized to ensure the accuracy with suitability of the CNN model training. The model was then trained on the available data using hyper-parameter tuning with iterative learning to enhance performance.

Table 1. 11x10 feature vector

Feature s	Classes										
	Healthy	S1 Open	S3 Open	S4 Open	S5 Open	S6 Open	S12 Open	S13 Open	S14 Open	S15 Open	S16 Open
median_x	-0.01	-0.11	-1.85	1.79	1.99	-1.97	-0.09	-1.70	0.56	1.93	-1.86
median_y	-0.03	-1.68	1.28	0.55	1.26	-1.17	0.00	-1.25	-2.54	-0.24	-2.20
points_x1	-0.01	-0.12	-1.85	1.79	1.99	-1.97	-0.10	-1.70	0.56	1.92	-1.89
points_y1	-4.16	-4.15	-2.24	0.53	-1.08	-2.97	0.00	-3.02	-4.56	-1.33	-1.69
points_x2	-0.01	-0.11	-1.85	1.79	1.99	-1.97	-0.09	-1.70	0.56	1.93	-1.86
points_y2	4.21	-0.66	3.79	0.57	2.98	1.17	0.00	-0.80	-1.50	0.07	-1.28
points_x3	3.99	2.74	-0.43	2.57	4.32	-0.07	2.03	-0.68	2.47	5.13	-0.09
points_y3	-0.03	-1.68	1.28	-0.45	1.26	-1.17	0.00	-1.26	-2.54	-0.24	-2.20
points_x4	-4.23	-3.21	-3.77	2.40	-0.10	-4.05	-0.98	-2.62	0.09	0.38	-3.97
points_y4	-0.03	-1.68	1.28	-0.52	1.25	-1.17	0.00	-1.25	-2.54	-0.24	-2.20

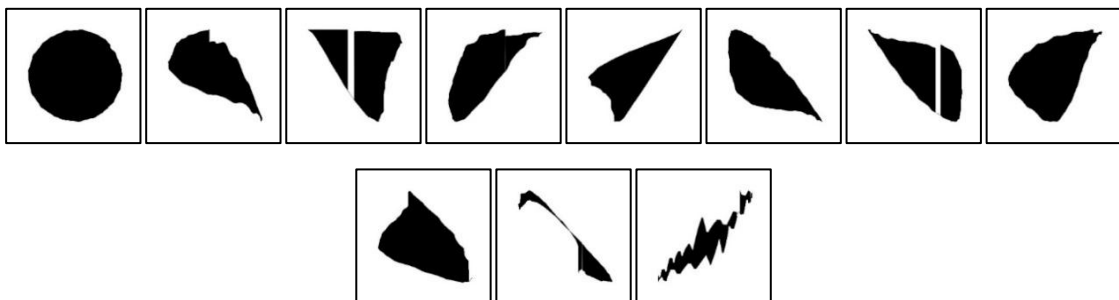


Fig. 8. Solid Images of Patterns

Table 2. If – Then Rule Base

Rule No.	Condition	Output
1)	$\text{median}_x = 0.0$ and $\text{median}_y = 0.0$	Healthy_Data
2)	$\text{median}_x < 0$ and $\text{median}_y < 0$ and $\text{points}_{x1} < 0$ and $\text{points}_{y1} < 0$ and $\text{points}_{x2} < 0$ and $\text{points}_{y2} < 0$ and $\text{points}_{y3} < 0$ and $\text{points}_{x4} < 0$ and $\text{points}_{y4} < 0$ and $\text{points}_{x3} > 0$	Open1

3)	$\text{median}_x < 0$ and $\text{points}_{x1} < 0$ and $\text{points}_{x2} < 0$ and $\text{points}_{x3} < 0$ and $\text{points}_{x4} < 0$ and $\text{median}_y > 0$ and $\text{points}_{y1} > 0$ and $\text{points}_{y2} > 0$ and $\text{points}_{y3} > 0$ and $\text{points}_{y4} > 0$	Open3
4)	$\text{median}_x > 0$ and $\text{median}_y > 0$ and $\text{points}_{x1} > 0$ and $\text{points}_{y1} > 0$ and $\text{points}_{x2} > 0$ and $\text{points}_{y2} > 0$ and $\text{points}_{x3} > 0$ and $\text{points}_{y3} < 0$ and $\text{points}_{y4} < 0$	Open4
5)	$\text{median}_x > 0$ and $\text{median}_y > 0$ and $\text{points}_{x1} > 0$ and $\text{points}_{y3} > 0$ and $\text{points}_{x2} > 0$ and $\text{points}_{y2} > 0$ and $\text{points}_{x3} > 0$ and $\text{points}_{y4} > 0$ and $\text{points}_{y1} < 0$ and $\text{points}_{x4} < 0$	Open5
6)	$\text{median}_x < 0$ and $\text{median}_y < 0$ and $\text{points}_{x1} < 0$ and $\text{points}_{y1} < 0$ and $\text{points}_{x2} < 0$ and $\text{points}_{x3} < 0$ and $\text{points}_{y3} < 0$ and $\text{points}_{x4} < 0$ and $\text{points}_{y4} < 0$ and $\text{points}_{y2} > 0$	Open6
7)	$\text{median}_y = 0$ and $\text{points}_{y1} = 0$ and $\text{points}_{y2} = 0$ and $\text{points}_{y3} = 0$ and $\text{points}_{y4} = 0$	Open12
8)	$\text{median}_x < 0$ and $\text{median}_y < 0$ and $\text{points}_{x1} < 0$ and $\text{points}_{y1} < 0$ and $\text{points}_{x2} < 0$ and $\text{points}_{y2} < 0$ and $\text{points}_{y3} < 0$ and $\text{points}_{x4} < 0$ and $\text{points}_{y4} < 0$ and $\text{points}_{x3} < 0$ and $\text{median}_x > -3.5$ and $\text{median}_y > -3.5$	Open13
9)	$\text{median}_y < 0$ and $\text{points}_{y1} < 0$ and $\text{points}_{y2} < 0$ and $\text{points}_{y3} < 0$ and $\text{points}_{y4} < 0$	Open14
10)	$\text{median}_x > 0$ and $\text{median}_y < 0$	Open15
11)	$\text{median}_x < 0$ and $\text{median}_y < 0$ and $\text{points}_{x1} < 0$ and $\text{points}_{y1} < 0$ and $\text{points}_{x2} < 0$ and $\text{points}_{y2} < 0$ and $\text{points}_{y3} < 0$ and $\text{points}_{x4} < 0$ and $\text{points}_{y4} < 0$ and $\text{points}_{x3} < 0$	Open16

RESULT & DISCUSSION

DQ-transformed features with median calculations were utilized for statistical feature-based fault diagnostic methods. Fault diagnosis enhances accuracy and efficiency by improving the definition and dependability of planned features by linking in-between calculations and DQ conversions. When applied to these features, Random Forest Classifier, Naïve Bayes, Support Vector Classifier (Non-Linear), and Support Vector Classifier (Linear) showed different levels of accuracy. The random forest classifier outperformed the linear and non-linear support vector classifiers by 42% and the naive Bayes (Gaussian) by 68%, with an accuracy of 98%.

The if-then rule-based approach promises accurate fault diagnosis with an impressive 99% accuracy rate. However, due to its rigid structure, which lacks flexibility and adaptability, this technique performed less well with noisy real-time inputs. SVCs and Naive Bayes perform less accurately due to their assumptions and limitations, but Random Forests perform better because they can capture complex relationships and are resistant to overfitting. However, the unpredictability of noisy inputs can be better handled by more flexible and adaptive methods, such as using ensemble methods or real-time learning processes.

After the standard feature extraction, the CNN and ML algorithms were trained on the sample images created by the DQ transformation. Images were Gray-scaled and resized to various resolutions to use as pre-processing steps. Traditional feature extraction methods included Gaussian and Sobel filters, max-pooling and data flattening. The Scale-Invariant Feature Transform (SIFT) and Speeded-Up Robust Features (SURF) approaches, which seek to locate and describe local features in pictures, can both be taken into consideration. ML algorithms such as Logistic Regression, Decision Tree Classifier and Random Forest Classifier were then applied, resulting in lower accuracy rates (12.8% to 20%) than the Statistical feature-based methods. Preprocessing techniques, cross-validation techniques, and hyperparameter tweaks to prevent overfitting or underfitting will also have an impact on an algorithm's accuracy. Using a CNN model, specifically ResNets, resulted in a significant improvement in accuracy of 87%, outperformed traditional ML methods. In comparison to conventional machine learning methods, ResNet enhances fault diagnosis and dramatically boosts classification accuracy by extracting complex, hierarchical characteristics from data using its deep structure and residual connections. Enhancing feature selection and applying domain-specific knowledge can improve the performance of ML algorithms.

ResNets, with its identity shortcut connections, allowed for the training of very deep networks while it mitigated the vanishing gradient problem and maintained robust performance.

Despite higher accuracy, image recognition was found to be less effective due to the complexity of multi-class

classification, longer diagnosis time and higher implementation effort. Table 3 shows that in terms of identifying open switch faults (OSFs) in voltage source inverters (VSIs), the statistical feature-based technique that used DQ-transformed data and central computation for feature selection performed better than the machine learning-based image. Identification technique. "Implementation effort" is evaluated as "moderate" if it requires moderate resources, manageable coding complexity and some parameter tuning, while "high" indicates significant resource demands, advanced coding, and the potential need for specialized hardware or domain expertise. The "robustness" of a method is scored as "moderate" if it performs consistently under normal conditions but falls short when exposed to high noise or unexpected data fluctuations, and is scored as "high" if it maintains accuracy in the face of varied noisy and unpredictable inputs.

The high accuracy of the Random Forest Classifier in the statistical feature-based methods demonstrated the efficacy of ensemble learning techniques in this domain. While the If-Then rule-based method was the most accurate, it was less flexible and ineffective with noisy real-time inputs which made it least robust technique. The ability of deep learning models to accurately identify complex patterns in altered photos was demonstrated through the application of ResNets in image identification. However, CNN's complexity, long diagnosis time, bad flexibility, and implementation difficulties make simplified statistical feature-based approaches more suitable for real-time problem diagnosis.

Table 3. Comparative analysis

Model	Accuracy (%)	Diagnostic Time	Implementation Effort	Robustness
Statistical feature-based methods for Fault Diagnosis				
ML Models				
a) Random Forest Classifier	98.0	Low	Medium	High
b) Naive Bayes (Gaussian)	68.0	Low	Medium	Medium
c) Support Vector Classifier (Non-Linear)	42.0	Low	Medium	Medium
d) Support Vector Classifier (Linear)	42.0	Low	Medium	Medium
If-Then Rule Base	99.0	Very Low	Low	Very Low
Image Recognition methods for Fault Diagnosis				
Training of ML Models				
(a) Logistic Regression	18.0	Medium	High	Medium
(b) Decision Tree Classifier	19.0	Medium	High	Medium
(c) Random Forest Classifier	20.0	Medium	High	High
Convolutional Neural Networks (CNN)				
ResNets	87.0	High	High	Medium

CONCLUSION AND FUTURE WORK

The identification of OSFs in 3 Φ -VSI, which are critical components in industrial settings, can be revolutionized by the innovative method revealed by our work. Accurate diagnosis is important to continue steady and useful processes in industrial settings as OSFs in 3 Φ -VSI can result into equipment breakdown, uselessness and expensive downtime. The statistical feature-based technique gives unique fault diagnosis performance, reducing downtime and safety risks by merging pattern recognition algorithms, direct quadrant transformation as well as a rigorous feature selection process. Pattern recognition algorithms, direct quadrant transformation and fine-grained feature selection allowed fast and correct fault diagnosis. This enhanced safety and significantly decreased downtime. This method was essential as, along with speeding up fault diagnosis, it was capable of avoiding the drawbacks of old diagnostic techniques. Low accuracy, rigidity, slow response time, noise sensitivity, low utilization of features as well as reliance on manual assessment, are certain of the drawbacks of traditional techniques that delay fault diagnosis. Poor robustness, expensive implementation, delayed diagnostic time and dependency on particular thresholds are all addressed by this technology. Accordingly, it delivered a robust way out that enhanced power electronic converter performance as well as reliability. Significantly, the proposed approach is fully compatible with the Industry 5.0 paradigm of condition-based monitoring and offers wide aids in several industrial sectors. This study optimizes power electronic converter maintenance procedures, increases efficiency, reduces downtime and improves safety in addition to guiding future

predictive maintenance and sophisticated diagnostic methods.

REFERENCES

- [1] Abid, M. *et al.* (2022) 'Diagnosis and localization of fault for a neutral point clamped inverter in wind energy conversion system using artificial neural network technique', *Electrical Engineering and Electromechanics*, 2022(5), pp. 55–59. Available at: <https://doi.org/10.20998/2074-272X.2022.5.09>.
- [2] Achintya, P. and Kumar Sahu, L. (2020) 'Open circuit switch fault detection in multilevel inverter topology using machine learning techniques', *PIICON 2020 - 9th IEEE Power India International Conference*, pp. 1–6. Available at: <https://doi.org/10.1109/PIICON49524.2020.9112870>.
- [3] Amol Rathod, Y. *et al.* (2022) 'Energy Meter Tamper Detection and Alert Messaging System', *International Journal of Technology Engineering Arts Mathematics Science*, 1(2), pp. 2583–1224. Available at: <https://doi.org/10.11591/eei.v9i3.xxxx>.
- [4] Basler, T. *et al.* (2013) 'Measurement of a complete HV IGBT I-V-characteristic up to the breakdown point', *2013 15th European Conference on Power Electronics and Applications, EPE 2013* [Preprint], (October 2015). Available at: <https://doi.org/10.1109/EPE.2013.6634454>.
- [5] Bengharbi, A.A. *et al.* (2023) 'Open-Circuit Fault Diagnosis for Three-Phase Inverter in Photovoltaic Solar Pumping System Using Neural Network and Neuro-Fuzzy Techniques', *Electrica*, 23(3), pp. 505–515. Available at: <https://doi.org/10.5152/electrica.2023.0141>.
- [6] Chen, C. *et al.* (2021) 'The Diagnostic Method for Open-Circuit Faults in Inverters Based on Extended State Observer', *Mathematical Problems in Engineering*, 2021. Available at: <https://doi.org/10.1155/2021/5526173>.
- [7] Chen, Y. *et al.* (2019) 'Faults and diagnosis methods of permanent magnet synchronous motors: A review', *Applied Sciences (Switzerland)*, 9(10). Available at: <https://doi.org/10.3390/app9102116>.
- [8] Dhumale, N.R. *et al.* (2024) 'Fuzzy Logic Diagnostics for Open-Circuit Faults in Renewable Energy Voltage Source Inverters with Changeable Load Conditions', *International Journal of Intelligent Systems and Applications in Engineering*, 12(1), pp. 80–86.
- [9] Farooqi, A. *et al.* (2022) 'Dynamic voltage restorer (DVR) enhancement in power quality mitigation with an adverse impact of unsymmetrical faults', *Energy Reports*, 8, pp. 871–882. Available at: <https://doi.org/10.1016/j.egyr.2021.11.147>.
- [10] Gong, W. *et al.* (2020) 'A Data-Driven-Based Fault Diagnosis Approach for Electrical Power DC-DC Inverter by Using Modified Convolutional Neural Network with Global Average Pooling and 2-D Feature Image', *IEEE Access*, 8, pp. 73677–73697. Available at: <https://doi.org/10.1109/ACCESS.2020.2988323>.
- [11] Mehta, P., Sahoo, S. and Dhiman, H. (2022) 'Open Circuit Fault Diagnosis in Five-Level Cascaded H-Bridge Inverter', *International Transactions on Electrical Energy Systems*, 2022, pp. 1–13. Available at: <https://doi.org/10.1155/2022/8588215>.
- [12] Sonawane, V. (2022) 'Comparative Study of Open Switch Fault diagnosis in Three Phase Voltage Source Inverter', 20(5), pp. 4865–4884. Available at: <https://doi.org/10.14704/nq.2022.20.5.NQ22763>.
- [13] Wu, F. and Zhao, J. (2016) 'A Real-Time Multiple Open-Circuit Fault Diagnosis Method in Voltage-Source-Inverter Fed Vector Controlled Drives', *IEEE Transactions on Power Electronics*, 31(2), pp. 1425–1437. Available at: <https://doi.org/10.1109/TPEL.2015.2422131>.